



HAL
open science

Master singular behavior from correlation length measurements for seven one-component fluids near their gas-liquid critical point

Yves Garrabos, Fabien Palencia, Carole Lecoutre-Chabot, Can John Erkey,
Bernard Le Neindre

► To cite this version:

Yves Garrabos, Fabien Palencia, Carole Lecoutre-Chabot, Can John Erkey, Bernard Le Neindre. Master singular behavior from correlation length measurements for seven one-component fluids near their gas-liquid critical point. *Physical Review E: Statistical, Nonlinear, and Soft Matter Physics*, 2006, 73 (2), 026125 (9 p.). 10.1103/PhysRevE.73.026125 . hal-00016105

HAL Id: hal-00016105

<https://hal.science/hal-00016105>

Submitted on 19 Dec 2005

HAL is a multi-disciplinary open access archive for the deposit and dissemination of scientific research documents, whether they are published or not. The documents may come from teaching and research institutions in France or abroad, or from public or private research centers.

L'archive ouverte pluridisciplinaire **HAL**, est destinée au dépôt et à la diffusion de documents scientifiques de niveau recherche, publiés ou non, émanant des établissements d'enseignement et de recherche français ou étrangers, des laboratoires publics ou privés.

Master singular behavior from correlation length measurements for seven one-component fluids near their gas-liquid critical point

Yves Garrabos*, Fabien Palencia, Carole Lecoutre, Can J. Erkey**
ESEME-CNRS, ICMCB-UPR 9048, Université Bordeaux 1,
87 avenue du Docteur Albert Schweitzer, F-33608 Pessac France. and
**on sabbatical leave from Department of Chemical Engineering,
University of Connecticut, Storrs, CT 06074 USA.*

Bernard Le Neindre

LIMHP-CNRS-UPR 1311, Université Paris 13, Avenue Jean Baptiste Clément, F-93430 Villetaneuse France.

(Dated: 27 July 2005)

We present the master (i.e. unique) behavior of the correlation length, as a function of the thermal field along the critical isochore, asymptotically close to the gas-liquid critical point of xenon, krypton, argon, helium 3, sulfur hexafluoride, carbon dioxide and heavy water. It is remarkable that this unicity extends to the correction-to-scaling terms. The critical parameter set which contains all the needed information to reveal the master behavior, is composed of four thermodynamic coordinates of the critical point and one adjustable parameter which accounts for quantum effects in the helium 3 case. We use a scale dilatation method applied to the relevant physical variables of the one-component fluid subclass, in analogy with the basic hypothesis of the renormalization theory. This master behavior for the correlation length satisfies hyperscaling. We finally estimate the thermal field extent, where the critical crossover of the singular thermodynamic and correlation functions deviate from the theoretical crossover function obtained from field theory.

PACS numbers: 64.60.-i, 05.70.Jk, 64.70.Fx

1. INTRODUCTION

Close to the gas-liquid critical point of a one-component fluid, the knowledge of the correlation length ξ , i.e. the size of the critical fluctuations of the order parameter, is one among the most important challenge to provide better critical phenomena understanding, in particular for hyperscaling and crossover descriptions. The correlation length measurements $\xi(\Delta T)$ as a function of the temperature distance $\Delta T = T - T_c$ to the critical point along the critical isochore $\rho = \rho_c$, in the homogeneous range $T > T_c$, have been published for Xe [1, 2], Kr [3], Ar [4], ^3He [5, 6], SF_6 [7, 8], CO_2 [9, 10], and D_2O [11, 12]. T (T_c) is the temperature (critical temperature). ρ (ρ_c) is the density (critical density). We report an analysis of these data using the scale dilatation method initially proposed by one of us [13, 14], which was recently upgraded [15] to account for quantum effects in light fluids such as ^3He . The basic information of the scale dilatation method is given by the four coordinates which localize the critical point on the experimental p (pressure), $v_{\bar{p}}$ (particle volume), T (temperature), phase surface. In addition, a single well-defined adjustable parameter, noted Λ_{qe}^* , characterizes the quantum contribution at $T \cong T_c$. Considering such a minimum set of critical parameters, the two main objectives of this paper are:

- i) to phenomenologically observe the master (i.e.

unique) singular behavior of the correlation length for the universality subclass of the one-component fluids. For this we simply use the appropriate scale dilatation of ΔT and ξ , showing the master behavior without exact knowledge of its singular functional form;

- ii) to fit the resulting master curve by a mean crossover function obtained from the recent results [16] of the massive renormalization scheme [17, 18, 19], valid for the complete universality class of the three-dimensional (3D) uniaxial symmetrical Ising like systems [20].

This paper is organized as follows. Section 2 provides the data sources. Only are considered the effective fitting results of the correlation length measurements which have been published in the litterature. After the introduction of the four critical coordinates which characterize each one-component fluid, we recall in Section 3 the essential features of the singular behavior of the correlation length. From a brief analysis based on the corresponding state scheme, we illustrate also the well-known failure of the classical theories of critical phenomena [21]. Section 4 presents the application of the scale dilatation method to the physical (field) variables of the fluid subclass, leading to the master singular behavior observed. A fitting (two-terms) power law equation, which satisfies universal features of asymptotic hyperscaling and (one-term) critical crossover valid in the preasymptotic domain [18], is also proposed in this Section 4. Then the fitting by a well-defined and complete mean crossover function obtained from the massive renormalization scheme, is made in Section 5. A brief analysis of the validity range of the classical-to-critical crossover description is given before concluding in Section 6.

*Electronic address: garrabos@icmcb-bordeaux.cnrs.fr

2. THE DATA SOURCES

The data sources are obtained from turbidity and scattering measurements as a function of T , which provide simultaneous determination of the susceptibility (proportional to the isothermal compressibility) and the correlation length. The measurements are performed “*near the critical point*”, that corresponds to a finite temperature range bounded by the max and min values of $\Delta T = T - T_{c,exp}$, where $T_{c,exp}$ is the measured (or estimated) critical temperature in the experiments. The relative precision estimated by the authors is generally of the order of 10%, but we have noted that the raw data for ξ , as a function of the raw data for ΔT , are scarcely given in the published results to provide easy control of this uncertainty level. The authors only have systematically reported their fitting results as a function of the dimensionless temperature distance $\Delta\tau^*$ to the critical point, defined by

$$\Delta\tau^* = \frac{\Delta T}{T_{c,exp}} = \frac{T - T_{c,exp}}{T_{c,exp}} \quad (1)$$

Such a normalized temperature difference is the relevant physical variable to describe the singular scaling behavior of the thermodynamic fluid properties along the critical isochore [22]. In the field theory framework [20], $\Delta\tau^*$ is proportional to the renormalized thermal field t of the $\Phi_{d=3}^4$ ($n = 1$)-model for the universality class considered in the present paper (see below) which corresponds to a scalar ($n = 1$) order parameter density and a three dimensional ($d = 3$) system.

The customary functional forms used to fit the data are:

- i) the effective (single term) power law divergence

$$\xi = \xi_0^+ (\Delta\tau^*)^{-\nu} \quad (2)$$

where the free amplitude ξ_0^+ is a fluid-dependent quantity and ν an effective critical exponent which only asymptotically ($\Delta\tau^* \rightarrow 0$) takes a universal theoretical value, estimated to $\nu_{Ising} \approx 0.63$ (see [23] for updated theoretical estimations). In Eq. (2), the value of the critical exponent can be considered as an adjustable parameter when measurements are performed in a restricted temperature range at finite distance to $T_{c,exp}$. The main characteristic of such fitting is the high correlation between the effective values of ξ_0^+ and ν , which are then highly dependent on $T_{c,exp}$ and on the (extension and mean) values of the temperature range covered by measurements.

ii) the Wegner expansion [24], generally restricted to the following (two-term) equation,

$$\xi = \xi_0^+ (\Delta\tau^*)^{-\nu} \left[1 + a_\xi^+ (\Delta\tau^*)^\Delta \right], \quad (3)$$

where $\Delta \approx 0.5$ is a universal critical exponent [23] which characterizes the leading family of the corrections to the

scaling behavior. a_ξ^+ is the fluid-dependent confluent amplitude of the first correction to scaling. In such a fitting equation, the exponents are generally fixed to their theoretical values, and only the adjustable amplitudes ξ_0^+ and a_ξ^+ remain highly correlated to $T_{c,exp}$. Moreover the contribution of the first confluent correction term to scaling mostly appears lower than - or of the same order of magnitude as - the experimental uncertainty (reflecting an effective experimental situation where $a_\xi^+ (> 0) \sim 1$ and $\Delta\tau^* \lesssim 10^{-2}$).

In Table I are summarized the selected fitting results [with free (or fixed) exponents and accounting (or not) for first-order Wegner term] for the seven fluids. All these fitting results are taken from literature (see references given in the last column of Table I).

3. ANALYSIS FROM THE CORRESPONDING STATE SCHEME

In Figure 1a (log-log scale; color online), are reported the curves illustrating the fitted singular behavior of the ξ (nm) raw data, as a function of $T - T_c$ (K) (from Eqs. (2) or (3) and data of Table 1). Each curve has an extension covering the experimental temperature range (while, at the Figure 1a scale, the curve thickness illustrates the 10% uncertainty on ξ measurements). The dimensional quantities make each fluid behavior clearly distinguishable (at the same value of $T - T_c = 40 mK$ for example, the ξ values are covering one decade: from $5 nm$ for 3He , up to $50 nm$ for D_2O).

Our first analysis starts from the following characteristic set [13, 14],

$$Q_{c,a_{\bar{p}}}^{min} = \left\{ T_c, v_{\bar{p},c}, p_c, \gamma'_c = \left[\left(\frac{\partial p}{\partial T} \right)_{v_{\bar{p},c}} \right]_{CP} \right\} \quad (4)$$

made of the four critical parameters needed to localize the critical point on the $p, v_{\bar{p}}, T$ phase surface. The selected data are given in Table II. The subscript c corresponds to the critical parameters, the subscript $a_{\bar{p}}$ recall the thermodynamic potential (see below) used to construct its associated phase surface, while the subscript \bar{p} corresponds to a quantity normalized per particle. The subscript CP means the value at the critical point. $v_{\bar{p}} = \frac{V}{N} = \frac{m_{\bar{p}}}{\rho}$, where V is the total volume of the fluid container, and N is the total amount of fluid particles of individual mass $m_{\bar{p}}$ [25]. Such a phase surface of equation $\Phi_{a_{\bar{p}}}^p(p, v_{\bar{p}}, T) = 0$ uses the two conjugated experimental variables, p (intensive) and V (extensive), and represents the fluid equilibrium states provided by the equation of state (e.o.s.) $p(T, v_{\bar{p}}) = - \left(\frac{\partial A}{\partial V} \right)_{T,N} = - \left(\frac{\partial a_{\bar{p}}}{\partial v_{\bar{p}}} \right)_T$ [26]. $A(\Omega_i)$ [$a_{\bar{p}}(\omega_i) = \frac{A}{N}$] is the total (per particle) Helmholtz free energy of natural variables $\Omega_i = (T, V, N)$ [$\omega_i = (T, v_{\bar{p}})$]. γ'_c is the common limiting direction at CP, in the $p; T$ plane, of both the critical isochore on the homogeneous (single phase) domain ($T > T_c$), and the satu-

Fluid	ξ_0^+ (Å)	ν	a_ξ^+	Δ	ΔT_{max} (K)	ΔT_{min} (K)	Ref.
<i>Xe</i>	2.0 ± 0.25	0.63 ± 0.05					[1]
<i>Xe</i>	1.84 ± 0.03	0.63 <i>fixed</i>	0.55	1/2 <i>fixed</i>	10	0.0026	[2]
<i>Kr</i>	1.71 ± 0.01	0.6304 <i>fixed</i>	0.624 ± 0.4	0.504 <i>fixed</i>	20	0.021	[3]
<i>Ar</i>	1.71 ± 0.25	0.63 ± 0.02			3.5	0.04	[4]
<i>Ar</i>	1.6 ± 0.2	0.64 ± 0.02			3.5	0.04	[4]
3He	4.8 ± 2.0	0.59 ± 0.04			0.00014	0.000014	[5]
3He	2.71 ± 0.015	0.629 ± 0.002	0.732 ± 0.007	0.502 ± 0.01	0.1	0.000014	[6]
<i>SF₆</i>	1.5 ± 0.23	0.67 ± 0.07			0.45	0.038	[7]
<i>SF₆</i>	2.016 ± 0.2	0.6214 ± 0.01			1.0	0.048	[8]
<i>CO₂</i>	1.94 ± 0.2	0.60 ± 0.02			10	0.01	[9]
<i>CO₂</i>	1.50 ± 0.09	0.633 ± 0.01			10	0.023	[10]
<i>D₂O</i>	1.30 ± 0.23	0.623 ± 0.03			13	0.15	[11]
<i>D₂O</i>	1.372 ± 0.01	0.6304 <i>fixed</i>	0.676 ± 0.2	0.504 <i>fixed</i>	22.	1.6	[12]

Table I: Published values of ξ_0^+ , ν , a_ξ^+ , and Δ , obtained from fitting [with the Eqs. (2,3)] the turbidity and scattering measurements, in the temperature range $\Delta T_{min} \leq T - T_c \leq \Delta T_{max}$, along the critical isochore of seven one-component fluids (for data sources and the selected fitting results see the references given in the last column).

ration pressure curve - [the projection of the vapor-liquid equilibrium state] - on the heterogeneous (two phase) domain ($T < T_c$). We note that the T_c values given in Table II, which result from complete thermodynamic analysis of the phase surface, are mostly different from $T_{c,exp}$, as the $\rho_c = \frac{m_{\bar{p}}}{v_{\bar{p},c}}$ values from Table II generally differ from the measured (or estimated) critical density in the selected experiments.

In a first step, from $Q_{c,a_{\bar{p}}}^{\min}$, we are able to derive dimensionless thermodynamic and correlation functions, using the scale factors,

$$(\beta_c)^{-1} = k_B T_c \quad (5)$$

as an energy unit, and

$$\alpha_c = \left(\frac{k_B T_c}{p_c} \right)^{\frac{1}{d}} \quad (6)$$

as a length unit. In regards to the noticeable differences in the ξ values observed in Figure 1a, at a same $T - T_c$ value, we note the small differences in α_c values, given in the column 8 of Table II. We also note that α_c , obtained only using intensive variables, is not dependent of the size $L \sim (V)^{\frac{1}{d}}$ of the container (k_B is the Boltzmann constant; $d = 3$). α_c has a clear physical meaning as a length unit [13]: it represents the spatial extent of the short-ranged (Lennard-Jones like) molecular interaction [27], which allows us to define $v_{c,I} = \frac{k_B T_c}{p_c}$ as the volume of the microscopic *critical interaction cell* of each fluid.

The introduction of the two characteristic dimension-

less numbers,

$$Z_c = \frac{p_c v_{\bar{p},c}}{k_B T_c} \quad (7)$$

and

$$Y_c = \gamma'_c \frac{T_c}{p_c} - 1 \quad (8)$$

allows us to rewrite the minimal set [Eq. (4)] in the more convenient form

$$Q_{c,a_{\bar{p}}}^{\min} = \left\{ (\beta_c)^{-1}, \alpha_c, Z_c, Y_c \right\} \quad (9)$$

which involves one energy scale factor, one length scale factor, and two dimensionless *scale factors* characterizing two preferred directions to cross the critical point along the critical isotherm and the critical isochore, respectively. Z_c is the usual critical compression factor. In addition, $(Z_c)^{-1} = n_c v_{c,I}$ is the number of particles that fill $v_{c,I}$, and *the minimal set given by the equation (9) appears related to the critical interaction cell properties.*

We recall that the critical compression factor Z_c , and the critical Riedel factor $\alpha_{R,c}$ - related to Y_c by $\alpha_{R,c} = Y_c + 1$ -, are also two basic tools for developing an e.o.s. for engineering fluid modeling.

Figure 1b (log-log scale; color online), gives the singular behavior of the dimensionless correlation length $\xi^* = \frac{\xi}{\alpha_c}$ as a function of the dimensionless temperature distance $\Delta\tau^*$ of Eq. (1), precisely obtained from the classical theory of corresponding states (here with two characteristic parameters), using $(\beta_c)^{-1}$ and α_c units.

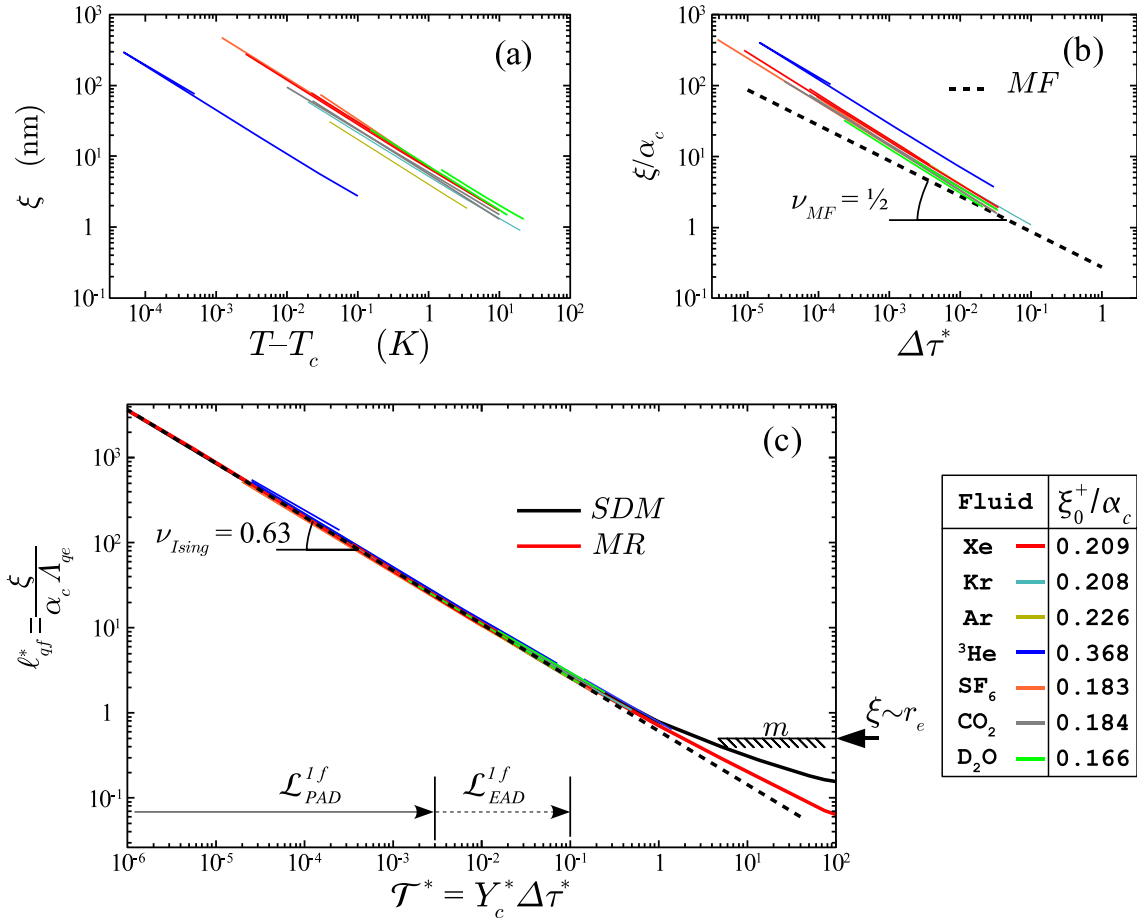


Figure 1: (Color online) a) Log-Log scale of ξ as a function of $T - T_c > 0$, along the critical isochore for Xe, Kr, Ar, ^3He , SF_6 , CO_2 , and D_2O . Each corresponding curve corresponds to the fit results reported in Table I, using Eqs. (2) and (3) for fitting data on the corresponding experimental range; b) Log-Log scale of the respective dimensionless variables expressed in α_c length unit and $(\beta_c)^{-1}$ energy unit, illustrating the failure of the classical corresponding state scheme. The expected mean field behavior with *classical* index $\nu_{MF} = \frac{1}{2}$ is given by the curve labelled *MF* [see text and Eq. (10)]; c) Matched master behavior (Log-Log scale) of the *renormalized* correlation length ℓ_{qf}^* , as a function of the *renormalized* thermal field \mathcal{T}^* , [see Eqs. (20) and (14), respectively]. The curves labelled *SDM* and *MR* correspond to the Eqs. (21) and (25), respectively. The dashed line illustrates the universal *critical* index $\nu_{Ising} \simeq 0.63$ for the asymptotic pure power law behavior of the uniaxial 3D Ising-like universality class. At large values of the renormalized thermal field ($\mathcal{T}^* \geq 3$), we have illustrated by the curve *m* a rough estimate $\ell_{qf}^* \approx \frac{1}{2}$ of the *microscopic* limit where the correlation length ξ will reach the order of magnitude of the two particle equilibrium position r_e (with $r_e \gtrsim \sigma$, where σ is the *size* of the particle); see text. In the superimposed Table are shown color indexation for each fluid (left column) and calculated $\frac{\xi_0^+}{\alpha_c}$ values (right column), using Eq. (28) and Table II data.

Fluid	$m_{\bar{p}}$ (10^{-26} kg)	Λ_{qe}^*	T_c (K)	$v_{\bar{p},c}$ (nm^3)	p_c (MPa)	γ'_c (MPa K^{-1})	$(\beta_c)^{-1}$ (10^{-21} J)	α_c (nm)	Z_c	Y_c
Xe	21.803	1	289.74	0.19589	5.84	0.118	4.0003	0.881508	0.28601	4.85434
Kr	13.9154	1	209.286	0.15292	5.5	0.1562	2.88951	0.806901	0.291065	4.94372
Ar	6.6336	1	150.725	0.12388	4.865	0.172	2.08099	0.753463	0.2896	4.32882
^3He	0.4983	1.11966	3.31555	0.12022	0.114724	0.11759	0.0457761	0.736198	0.301284	2.39837
SF_6	24.252	1	318.70	0.32684	3.76	0.0835	4.4	1.054	0.281	6.08
CO_2	7.308	1	304.14	0.15622	7.3753	0.170	4.2	0.829	0.274	6.01
D_2O	3.329	1	643.89	0.09346	21.671	0.2717	8.88987	0.743029	0.227829	7.07277

Table II: Minimal set of critical parameters [see Eqs. (4) and (9)] for the seven one-component fluids of particle mass $m_{\bar{p}}$. $\Lambda_{qe}^* \geq 1$ [Eq. (17)] differs from unity by a nonuniversal adjustable quantity proper to the nature of the ^3He quantum particle [see text and Eqs (18) and (19)]

Evaluation from standard mono-atomic Xe, shows the failure of the classical theory, *increasing* quantum effects in ^3He , and *decreasing* non-spherical interaction effects in D_2O . The dimensionless correlation length is then covering a relative variation by a factor more than 2 at the same reduced temperature distance to the critical point (see also our calculated values of $\frac{\xi_0^+}{\alpha_c}$ in the inserted table on Figure 1). Moreover an illustration of the inaptness of the “mean field” exponent $\nu_{MF} = \frac{1}{2}$ to describe the *classical* fluctuation behavior [28] expected from Van der Waals-like theories, is shown by the curve labelled *MF*, of equation

$$\frac{\xi_{MF}}{\alpha_c} = \frac{1}{4} \left(\frac{3\sqrt{2}}{\pi} \right)^{\frac{1}{d}} (\Delta\tau^*)^{-\nu_{MF}} \quad (10)$$

We note also that the classical approach along the critical isochore in the homogeneous domain is not able to reproduce experimental behavior at large distance to the critical point. Such a failure can be related to the number of interacting particles (here given by $\frac{1}{Z_c} \sim 3-4$), which seems too small to validate a “mean field approximation” of the attractive molecular interaction at distance greater than α_c for a fluid at critical density, as we will discuss below (see Section 5).

4. ANALYSIS USING THE SCALE DILATATION METHOD

As demonstrated in references [14, 29], Z_c and Y_c can be used as the two scale factors to formulate the dimensionless master asymptotic behavior of the one component fluid subclass. As a matter of fact, asymptotic master singular behaviors of dimensionless potentials and dimensionless correlation functions only occur [13] using appropriate dilatations of the following physical variables,

$$\Delta\tau^* = k_B\beta_c(T - T_c) \quad (11)$$

(to generate the *renormalized* thermal field),

$$\Delta h^* = \beta_c(\mu_{\bar{p}} - \mu_{\bar{p},c}) \quad (12)$$

(to generate the *renormalized* ordering field), and

$$\Delta m^* = (\alpha_c)^d (n - n_c) \quad (13)$$

(to generate density of the *renormalized* order parameter - conjugated to the *renormalized* ordering field). These scale dilatations of the fluid variables are now defined [15] in complete formal analogy to the field theory framework [20]. Such a theoretical approach provides a comprehensive understanding of the diverging universal character of the spontaneous fluctuations of extensive variables, using the renormalization group (RG) techniques [30, 31, 32], to deal with the contributions

of *critical* fluctuations. We briefly recall that this theoretical approach accounts for infinite degrees of freedom near the non-Gaussian (Wilson-Fisher) fixed point, throughout the Landau-Ginzburg-Wilson Hamiltonian of the $\Phi_{d=3}^4$ ($n=1$)-model for the universality class of the 3D uniaxial symmetrical Ising like systems, with associated coupling constant $u_4 > 0$. In this model, the relevant pair of renormalized fields are the weakly fluctuating thermal field t , and the ordering field h which exhibits stronger fluctuations, with $\{t=0, h=0\}$ at the isolated non-Gaussian fixed point. A single parameter κ , such that $\kappa \ll \Lambda_0$, measures the distance to the non-Gaussian fixed point in such a way that this fixed point corresponds to $\kappa^* = \frac{\kappa}{\Lambda_0} = 0$. Λ_0 is the actual microscopic wave number, characterizing a discrete structure of matter with spacing $(\Lambda_0)^{-1}$. κ is precisely related to the inverse correlation length ξ^{-1} of the fluctuations of the order-parameter m , conjugated to h , with $\ell_{qf}^* = \Lambda_0\xi = (\kappa^*)^{-1}$. Here ℓ_{qf}^* corresponds to the dimensionless form of the actual fluid correlation length expressed in units of α_c [Eq. (6)], also including quantum fluids (labelled qf) throughout the introduction of a dimensionless adjustable parameter Λ_{qe}^* which account for the quantum effects [see below the Eq. (20) and the related discussion]. At the fixed point, the fluctuations are *infinite*, i.e. $\xi(t=0, h=0) \sim \infty$. Close to the non-Gaussian fixed point within the critical asymptotic domain, i. e. for small values of the renormalized fields t and h which ensure that $\kappa \ll \Lambda_0$, the Wegner expansions [24] represent the singular behavior of thermodynamics and correlations functions of any physical system belonging to the universality class of this $\Phi_{d=3}^4$ ($n=1$)-model. In particular, the Wegner expansion of Equation (3) can be used for ξ . In that critical asymptotic domain, ξ , although *finite*, is still larger than $(\Lambda_0)^{-1}$. So that the close critical vicinity of the non-Gaussian fixed point can be defined by $\ell_{qf}^* = \Lambda_0\xi \gg 1$.

The renormalization introduces the two-scale universality of the physical system through analytical proportionality between the physical variables and the renormalized fields t and h , respectively [30, 31]. In a similar manner, the scale dilatation method is defined by the following *renormalization* of $\Delta\tau^*$ and Δh^* into \mathcal{T}_{qf}^* and \mathcal{H}_{qf}^*

$$\mathcal{T}_{qf}^* \equiv \mathcal{T}^* = Y_c\Delta\tau^* \quad (14)$$

$$\mathcal{H}_{qf}^* = (\Lambda_{qe}^*)^2 \mathcal{H}^* = (\Lambda_{qe}^*)^2 (Z_c)^{-\frac{d}{2}} \Delta h^* \quad (15)$$

respectively. Correspondingly, the *renormalization* of the order parameter Δm^* into \mathcal{M}_{qf}^* reads as follows

$$\mathcal{M}_{qf}^* = \Lambda_{qe}^* \mathcal{M}^* = \Lambda_{qe}^* (Z_c)^{\frac{d}{2}} \Delta m^* \quad (16)$$

Obviously, \mathcal{T}^* , \mathcal{H}^* and \mathcal{M}^* , are the renormalized variables defined for non-quantum fluids, for which the

nonuniversal wave number reads $\Lambda_0 = \frac{1}{\alpha_c}$, since α_c is the single explicit length unit. In Eq. (14), the identity $T_{qf}^* \equiv T^*$ means that the quantum effects are only accounted for at $T \cong T_c$. In Eqs. (15) and (16), the dimensionless parameter

$$\Lambda_{qe}^* = 1 + \lambda_c \quad (17)$$

accounts for quantum effects on the microscopic wave number Λ_0 at $T \cong T_c$ [15], in such a relative phenomenological way that

$$\Lambda_0 \Lambda_{qe}^* = \frac{1}{\alpha_c} \quad (18)$$

with

$$\lambda_c = \lambda_{q,f} \frac{\Lambda_{T,c}}{\alpha_c} \quad (19)$$

$\lambda_{q,f}$ (with $\lambda_{q,f} > 0$), is thus a nonuniversal adjustable number which accounts for statistical contribution due to the nature (boson, fermion, etc.) of the quantum particle. $\Lambda_{T,c} = \frac{h_P}{(2\pi m_{\bar{p}} k_B T_c)^{\frac{1}{2}}}$ is the de Broglie thermal wavelength at $T = T_c$, h_P is the Planck constant (the subscript P is here added to make a distinction with the field theory ordering field h). The Eq. (18) preserves the same length scale unit for thermodynamic and correlations functions.

Therefore, the *renormalized* dimensionless correlation length is given by

$$\ell_{qf}^* = (\kappa^*)^{-1} = \Lambda_0 \xi = \frac{\xi^*}{\Lambda_{qe}^*} = \frac{\xi}{\alpha_c \Lambda_{qe}^*} \quad (20)$$

and the corresponding dilatation of the dimensionless axis $\Delta\tau^*$ and $\frac{\xi}{\alpha_c}$ into \mathcal{T}^* and ℓ_{qf}^* are then defined by Eqs. (14) and (20), respectively, only using $Q_{c,a\bar{p}}^{\min}$ and Λ_{qe}^* .

The expected collapsing onto the master behavior obtained from application of this scale dilatation method to the physical variables is shown in Figure 1c (log-log scale; color online), *independently of any theoretical form used to represent this master behavior*. The scatter between the curves now corresponds to their estimated precision (10%) for each fluid correlation length.

Since the scale dilatation of the physical variables [see equations (14) and (15)] is analogous to the basic hypotheses of the renormalization group, we expect that the master asymptotic singularities present the universal features of the universality class. Specially within the preasymptotic domain, the observed divergence of ℓ_{qf}^* can be represented by the following two-term Wegner expansion

$$\ell_{qf}^* = Z_{\xi}^+ (\mathcal{T}^*)^{-\nu} \left[1 + Z_{\xi}^{1,+} (\mathcal{T}^*)^{\Delta} \right] \quad (21)$$

where the leading amplitude $Z_{\xi}^+ = 0.57$ and the first confluent amplitude $Z_{\xi}^{1,+} = 0.377$ have *master* (i.e. constant) values for the pure fluid subclass (see the Refs.

	exponent	Z_{ξ}^+	S_2	i	$X_{\xi,i}$	$Y_{\xi,i}$
ν	0.6303875	2.121008	22.9007	1	40.0606	-0.098968
Δ	0.50189			2	11.9321	-0.15391
Δ_{MF}	0.5			3	1.90235	-0.00789505
					$Z_{\xi}^{1,+}$	5.81623

Table III: Values of the universal exponents and constant parameters of Eqs. (22), (23) and (30).

[14, 29] for details making reference to critical xenon behavior [33] in order to obtain these master values). This result, obtained from master singular behavior of thermodynamic properties satisfies asymptotic hyperscaling and extends the scaling assertions first proposed by Widom [22] for the equation of state of the one-component fluid.

5. MEAN CROSSOVER FUNCTION FROM THE MASSIVE RENORMALIZATION SCHEME

We can now consider the “min” and “max” accurate expressions of the complete classical-to-critical crossover recently proposed by Bagnuls and Bervillier [16]. From the numeric values of the parameters of the generic functions $F_{min}(t)$ and $F_{max}(t)$ given in Tables I and II of reference [16], we have derived the numerical values of parameters associated to the mean crossover functions which reproduce as closely as possible the error treatment initially made by the authors from their generic functions. Such a mean crossover function for the inverse correlation length reads as follows

$$[\ell^*(t)]^{-1} = Z_{\xi}^+ (t)^{\nu} \prod_{i=1}^{i=3} \left[1 + X_{\xi,i} t^{D(t)} \right]^{Y_{\xi,i}} \quad (22)$$

with

$$D(t) = \frac{\Delta + \Delta_{MF} S_2 \sqrt{t}}{1 + S_2 \sqrt{t}} \quad (23)$$

and

$$t = \vartheta |\Delta\tau^*| \quad (24)$$

All the critical exponents (ν , Δ , Δ_{MF}) and the constants (Z_{ξ}^+ , $X_{\xi,i}$, $Y_{\xi,i}$, S_2) are given in Table III. The adjustable parameter ϑ introduces the non-universality proper to each selected system.

To fit each curve of Figure 1a with equations (22) to (24), we introduce one asymptotic (system-dependent) prefactor λ_0 , of dimension $[length]^{-1}$, from the following equation

$$\frac{1}{\xi(\Delta\tau^*)} = \lambda_0 Z_{\xi}^+ (\Delta\tau^*)^{\nu} \prod_{i=1}^{i=3} \left[1 + X_{\xi,i} t^{D(t)} \right]^{Y_{\xi,i}} \quad (25)$$

where we note that the leading term is now a unique function of $\Delta\tau^*$, as proposed by Bagnuls and Bervillier

[16]. In such a fitting procedure, ϑ is readily seen as a crossover parameter associated with one irrelevant physical field. The prefactor λ_0 satisfies to the two-scale universal feature of this universality class, associated with the two relevant physical fields (only two among all these prefactors are characteristics of the non-universality of the selected system). From our definition of the length unit, we can rewrite λ_0 as follows

$$\lambda_0 = \frac{1}{\alpha_c} \ell_0^* \quad (26)$$

leading to the following modification of the above equation (25)

$$\frac{\alpha_c}{\xi(\Delta\tau^*)} = \ell_0^* \mathbb{Z}_\xi^+ (\Delta\tau^*)^\nu \prod_{i=1}^{i=3} \left[1 + X_{\xi,i} t^{D(t^*)} \right]^{Y_{\xi,i}} \quad (27)$$

Now it is easy to understand that the restricted analysis of the two-term Wegner expansion provides complete materials for the unequivocal determination of the two adjustable parameters ℓ_0^* and ϑ . For example, the asymptotic term to term comparison of equation (3) and inverse equation (27), provides the following two relations

$$\xi_0^+ = \alpha_c \left(\ell_0^* \mathbb{Z}_\xi^+ \right)^{-1} \quad (28)$$

and

$$a_\xi^+ = \mathbb{Z}_\xi^{1,+} (\vartheta)^\Delta \quad (29)$$

where

$$\mathbb{Z}_\xi^{1,+} = - \sum_{i=1}^{i=3} X_{\xi,i} Y_{\xi,i} \quad (30)$$

The value of the constant amplitude $\mathbb{Z}_\xi^{1,+}$ is given in Table III. However, we note that the quantum correction parameter disappears in such a *standard* estimation of the leading prefactor (and leading amplitude) when the two scale factors are unknown [33].

From the scale dilatation method, to fit the master curve of Figure 1c with equations (22) to (24), need to introduce two master (i.e. constant) parameters, $\ell_0^{\{1f\}}$ and $\vartheta^{\{1f\}}$, that are characteristics of the one-component fluid subclass, using the crossover modeling equation

$$\frac{1}{\ell_{qf}^*(\mathcal{T}^*)} = \ell_0^{\{1f\}} \mathbb{Z}_\xi^+ (\vartheta^{\{1f\}} \mathcal{T}^*)^\nu \times \prod_{i=1}^{i=3} \left[1 + X_{\xi,i} (\vartheta^{\{1f\}} \mathcal{T}^*)^{D(\vartheta^{\{1f\}} \mathcal{T}^*)} \right]^{Y_{\xi,i}} \quad (31)$$

In equation (31),

$$\ell_0^{\{1f\}} = \left[\mathbb{Z}_\xi^+ \mathbb{Z}_\xi^+ (\vartheta^{\{1f\}})^\nu \right]^{-1} \quad (32)$$

and

$$\vartheta^{\{1f\}} = \left(\frac{\mathbb{Z}_\xi^{1,+}}{\mathbb{Z}_\xi^+} \right)^{\frac{1}{\Delta}} \quad (33)$$

in order to agree with the two-term asymptotic behavior given by equation (21). The mandatory relation between the relevant field t of the $\Phi_{d=3}^4(1)$ -model and the master field \mathcal{T}^* of the fluid subclass reads as follows

$$t = \vartheta^{\{1f\}} \mathcal{T}^* \quad (34)$$

From \mathbb{Z}_ξ^+ , $\mathbb{Z}_\xi^{1,+}$, \mathbb{Z}_ξ^+ , and $\mathbb{Z}_\xi^{1,+}$ values we obtain $\vartheta^{\{1f\}} = 0.004288$ and $\ell_0^{\{1f\}} = 25.699$. We note that the *master prefactor* $\ell_0^{\{1f\}}$ is attached to the correlation length behaviors above and below the critical temperature, while the *master crossover parameter* $\vartheta^{\{1f\}}$ is the same for any property along the critical isochore, above and below the critical temperature. The respective curves labelled *SDM* [of equation (21)] and *MR* [of inverse equation (31)], are illustrated in Figure 1c, with noticeable asymptotic agreement with master experimental behavior of the seven one-component fluids. The preasymptotic domain (labelled *PAD*), described by a Wegner expansion restricted to the first confluent correction [see equation (21)], extends up to $\mathcal{L}_{PAD}^{1f} \lesssim 3 \cdot 10^{-3}$ (see the corresponding arrow in \mathcal{T}^* axis). In the extended asymptotic domain (labelled *EAD*) which extends up to $\mathcal{L}_{EAD}^{1f} \lesssim 0.1$ (see the corresponding arrow in \mathcal{T}^* axis), the observed master behavior is well-represented by the theoretical critical-to-classical crossover [see equation (31)]. From the comparison of Figures 1b and 1c, we can also note that the applicability of the two-scale master behavior obtained from the scale dilatation method goes far beyond the applicability of the corresponding state method based on classical theory.

By reversing the scale dilatation method for any one-component fluid where Q_{c,a_p}^{\min} and Λ_{qe}^* are known, it is easy to determine its attached two characteristic parameters ℓ_0^* and ϑ , and to derive Eq. (3) from Eq. (21), using the following relations

$$\ell_0^* = \frac{1}{\Lambda_{qe}^*} \ell_0^{\{1f\}} \quad (35)$$

$$\vartheta = Y_c \vartheta^{\{1f\}} \quad (36)$$

$$\xi_0^+ = \alpha_c \Lambda_{qe}^* (Y_c)^{-\nu} \mathbb{Z}_\xi^+ \quad (37)$$

$$a_\xi^+ = \mathbb{Z}_\xi^{1,+} (Y_c)^\Delta \quad (38)$$

Equation (3) can now be readily used without any adjustable parameter (except Λ_{qe}^*).

Since the critical behaviour predicted by RG theory asymptotically agrees with the master behavior for the one-component fluid subclass, the only remaining problem is the determination of the thermal field distance at which significant deviation between the $\Phi_{d=3}^4$ ($n=1$)-model and the fluid subclass appears. To point out that such a thermal distance (noted \mathcal{T}_{CO}^* in the following) exists, we consider the variation of the effective exponent, $\nu_{eff} = -\frac{d\ln(\ell_{qf}^*)}{d\ln\mathcal{T}^*}$, as a function of \mathcal{T}^* . In addition, it is also possible to consider the variation of the effective exponent, $\gamma_{eff} = -\frac{d\ln(\chi_{qf}^*)}{d\ln\mathcal{T}^*}$, which is now entirely known [34], thanks to universal features predicted by RG theory and definitions [see equations (14), (15), and (16)] of the scale dilatation. $\chi_{qf}^*(\mathcal{T}) = \left(\frac{\partial\mathcal{M}_{qf}^*}{\partial\mathcal{H}_{qf}^*}\right)_{\mathcal{T}} = (\Lambda_{qe}^*)^{2-d} (Z_c)^{d-2} \kappa_T^*$ is the renormalized susceptibility [15], with $\kappa_T^* = p_c \kappa_T$. $\kappa_T = \frac{1}{\rho} \left(\frac{\partial\rho}{\partial T}\right)_T$ is the (physical) isothermal compressibility. The two limits for the γ_{eff} -variation calculated from the $\Phi_{d=3}^4$ (1)-model are $\gamma_{MF} = 1$ (close to the Gaussian fixed point) and $\gamma_{Ising} \cong 1.24$ [23] (close to the Wilson-Fisher fixed point).

The complete results are shown in Figure 2 (color online) as a function of the renormalized thermal field \mathcal{T}^* (lower axis), or as a function of the renormalized correlation length ℓ_{qf}^* (upper axis). We recall that ℓ_{qf}^* gives a best estimate of the ratio between the effective size (ξ) of the critical fluctuations and the effective size (α_c) of the attractive molecular interaction. Since the typical range of the dispersion forces in Lennard-Jones-like fluids is slightly greater than twice the equilibrium distance ($r_e \gtrsim \sigma$) between two interacting particles of finite core size σ , we have reported on the upper axis of Figure 2 a rough estimate [$\ell_{qf}^* \approx \frac{1}{2}$] of the limit where the correlation length will be comparable with the order of magnitude of the particle size. From the theoretical crossover fit, such a limit corresponds to $\mathcal{T}_{\bar{p}}^* \approx 1.3$ (here the superscript \bar{p} is for a related particle property). Therefore, it is important to note that the effective crossover for the fluid subclass appears in the thermal field range $\mathcal{T}_{CO}^* \approx 0.5 - 1$ where $\ell_{qf}^* \lesssim 1$, as discussed below.

As illustrated by the curve labelled *CO* in Figure 2a, the rough estimate of the effective crossover around $\mathcal{T}_{CO}^* \approx 0.5 - 1$ corresponds to the following noticeable differences in γ_{eff} -values obtained from fitting analyses [13, 35, 36, 37] of the isothermal compressibility data of xenon obtained from pVT measurements [38, 39, 40]: for $\mathcal{T}^* < \mathcal{T}_{CO}^*$, γ_{eff} -values are always greater than $\frac{\gamma_{Ising} + \gamma_{MF}}{2} \cong 1.12$ and increase to $\gamma_{Ising} \cong 1.24$ when $\mathcal{T}^* \rightarrow 0$; for $\mathcal{T}^* \geq \mathcal{T}_{CO}^*$, γ_{eff} -value is slightly constant and close to unity (see also the Figure 1 in reference [33]). This general trend is observed whatever the selected pure fluid, as already noted in references [13, 14]. In spite of the difficulty in determining the precise shape of the γ_{eff} -variation in this crossover range where $\ell_{qf}^* \lesssim 1$, we may expect to not observe a collapse onto an unique crossover

curve for different pure fluids (see also our analysis [29] of crossover behavior for the renormalized order parameter of several pure fluids in the non-homogeneous domain). As a matter of fact, the massive renormalization scheme is not appropriate when $\ell_{qf}^* \lesssim 1$. We have illustrated this situation by the hypothetical curves labelled *CO* and *8* in Figure 2b where a possible decrease of ν_{eff} to zero occurs crossing \mathcal{T}_{CO}^* . Such a zero-value [significantly different from the (mean-field) $\frac{1}{2}$ -value] should be the result of an expected value $\ell_{qf}^* = const \cong \frac{1}{2}$ (see the limiting curve *m*, analogous to the one of Figure 1) related to a constant value of the direct correlation length (however, as already noted, $\ell_{qf}^* \approx \frac{1}{2}$ is not here a “master” value whatever the pure fluid). At large temperature distance to the critical point (i.e. for $\mathcal{T} \gg \mathcal{T}_{CO}$), such a limit means that the direct correlation between interacting particles at equilibrium position ($r_e \cong \frac{\alpha_c}{2}$) inside the (short-ranged) critical interaction cell, can mainly contribute to the local density fluctuations. We recall that, along the critical isochore in the homogeneous phase, $\frac{1}{Z_c}$, i.e. the number of particle in the critical interaction cell, and α_c , i.e. the size of the critical interaction cell, are two quantities which are slightly dependent on the temperature range (since the critical isochore is closely a straight line in the $p; T$ diagram). Such a conjectured microscopic situation is realistic and similar to the results obtained from molecular numerical simulation of a Lennard-Jones like fluid, precisely in the temperature range $T^* = \frac{k_B T}{\varepsilon_{LJ}} > 2$ (which corresponds to $T^* > 1.5$ for the monoatomic rare gases such as argon, krypton and xenon). In that situation, only the first peak of the static structure factor is observed to be significant in a reduced density [$\rho^* = \frac{\rho(\sigma_{LJ})^d}{m_{\bar{p}}} \approx 0.3$] range including the reduced critical density $\rho_c^* \approx 0.3$ (ε_{LJ} and σ_{LJ} are the two characteristics parameters of the Lennard-Jones like potential). However, at such “low” density and “high” temperature ranges, the associated coordination number ($\lesssim 4$) is too small to infer validity of a mean-field approximation of the attractive interaction.

6. CONCLUSION

We provide an asymptotic description for the correlation length singular behavior of the one-component fluid subclass. The master critical crossover behavior of this subclass can be observed up to $\mathcal{T}^* \approx 0.1$ (or $\ell_{qf}^* \approx 3$). The one-component fluid subclass then corresponds to the simplest situation in the $\Phi_{d=3}^4$ ($n=1$)-model where the starting point for $u_4 > 0$ (in usual renormalized trajectories [32]), is certainly very close to the ideal RG trajectory between the Gaussian and the Wilson-Fisher fixed points [32]). Such a supplementary constraint, is not a necessity in the field theory framework [16]. In a complementary work, we will show that this constraint certainly takes origin in the description of the critical point vicinity by *finite* (linearized) ther-

modynamics, which provides complete understanding for the *master* thermodynamic properties normalized at the

volume scale $(\alpha_c)^d$ of the critical interaction cell.

-
- [1] H. L. Swinney and D. L. Henry, Phys. Rev. A **8**, 2586 (1973).
- [2] H. Güttinger and D. S. Cannell, Phys. Rev. A **24**, 3188 (1981).
- [3] M. Bonetti, P. Calmettes, and C. Bervillier, J. Chem. Phys. **119**, 8542 (2003).
- [4] J. S. Lin and P. W. Schmidt, Phys. Rev. Lett. **33**, 1265 (1974); Phys. Rev. A **10**, 2290 (1974).
- [5] K. Ohbayashi and A. Ikushima, Phys. Lett. **46A**, 131 (1973).
- [6] F. Zhong, M. Barmatz, and I. Hahn, Phys. Rev. E **67**, 021106 (2003).
- [7] V. G. Puglielli and N. C. Ford, Jr., Phys. Rev. Lett. **25**, 143 (1970).
- [8] D. S. Cannell, Phys. Rev. A **12**, 225 (1975).
- [9] B. S. Maccabee and J. A. White, Phys. Rev. Lett. **27**, 495 (1971).
- [10] J. H. Lunacek and D. S. Cannell, Phys. Rev. Lett. **27**, 841 (1971).
- [11] D. Sullivan, PhD Thesis, University of Bristol, 2000, unpublished.
- [12] M. Bonetti, G. Romet-Lemonne, P. Calmettes, and M.C. Bellissent-Funel, J. Chem. Phys. **112**, 268 (2000).
- [13] Y. Garrabos, Thesis, University of Paris VI, 1982, unpublished.
- [14] Y. Garrabos, J. Phys. (France) **44**, 281-291 (1985) [for an english version see <https://hal.ccsd.cnrs.fr/ccsd-00015956> (15 Dec. 2005) or <http://fr.arxiv.org/abs/cond-mat/0512347>]; **45**, 197-206 (1986).
- [15] Y. Garrabos, *Preprint* 2005 [see <https://hal.ccsd.cnrs.fr/ccsd-00015988> (16 Dec. 2005) or <http://fr.arxiv.org/abs/cond-mat/0512408>].
- [16] C. Bagnuls and C. Bervillier, Phys. Rev. E **65**, 066132 (2002).
- [17] C. Bagnuls and C. Bervillier, J. Phys. (France) - Lettres **45**, L-95 (1984).
- [18] C. Bagnuls and C. Bervillier, Phys. Rev. B **32**, 7209 (1985).
- [19] C. Bagnuls, C. Bervillier, D. I. Meiron, and B.G. Nickel, Phys. Rev. B **35**, 3585 (1987); **65**, 149901(E) (2002).
- [20] see for example J. Zinn-Justin, *Euclidean Field Theory and Critical Phenomena*, 3rd ed. (Oxford University Press, 1996).
- [21] see for example M. A. Anisimov and J. V. Sengers, Critical Region, in “*Equations of state for fluids and fluid mixtures*”. Part I, Ed. J. V. Sengers, R. F. Kayser, C. J. Peters, and H. J. White, Jr. (Elsevier, Amsterdam, The Netherlands, 2000) pp. 381-434.
- [22] B. Widom, J. Chem. Phys. **43**, 3898 (1965).
- [23] R. Guida and J. Zinn-Justin, J. Phys. A: Math. Gen. **31**, 8103 (1998).
- [24] F. J. Wegner, Phys. Rev. B **5**, 4529-4536 (1972).
- [25] We admit that the molecular mass, $m_{\bar{p}}$, of each constitutive fluid particle is a known quantity, in order to infer N value from total mass ($M = Nm_{\bar{p}}$) measurement of the amount of fluid matter filling the container of measured total volume V .
- [26] see for example M. Modell and R. C. Reid, *Thermodynamics and its Applications*. 2nd ed. (Prentice Hall, New York, 1983).
- [27] J. O. Hirschfelder, C. F. Curtiss, and R. B. Bird, *Molecular Theory of Gases and Liquids* (corrected edition), (Wiley, New York, 1964).
- [28] A. Kostrowicka Wyczalkowska, J. V. Sengers, and M. A. Anisimov, Physica A **334**, 482 (2004).
- [29] Y. Garrabos, B. Le Neindre, R. Wunenburger, C. Lecoutre-Chabot, and D. Beysens, Int. J. Thermophys. **23**, 997 (2002).
- [30] K. G. Wilson, Phys. Rev. B **4**, 3174 (1971).
- [31] K. G. Wilson and J. Kogut, Phys. Rep. C **12**, 75 (1974).
- [32] see for example, C. Bagnuls and C. Bervillier, Cond. Matter Phys. **3**, 559-575 (2000), and references therein.
- [33] C. Bagnuls, C. Bervillier, and Y. Garrabos, J. Phys. (France)- Lettres **45**, L-127 (1984).
- [34] Y. Garrabos, F. Palencia, C. Lecoutre, and C. Bervillier, preprint (2005).
- [35] W. T. Estler, R. Hocken, T. Charlton, and L. R. Wilcox, Phys. Rev. A **12**, 2118 (1975); R. J. Hocken and M. R. Moldover, Phys. Rev. Lett. **37**, 29 (1976).
- [36] J. V. Sengers and M. R. Moldover, Phys. Lett. **66A**, 44 (1978).
- [37] J. M. H. Levelt-Sengers, W. L. Greer, and J. V. Sengers, J. Phys. Chem., **5**, 1 (1976).
- [38] H. W. Habgood and W. G. Schneider, Can. J. Chem. **32**, 98 (1954).
- [39] A. Michels, T. Wassenaar, and P. Louwerse, Physica **20**, 99 (1954).
- [40] J. A. Beattie, R. J. Barriault, and J. S. Brierley, J. Chem. Phys. **19**, 1219 (1951); **19**, 1222 (1951).

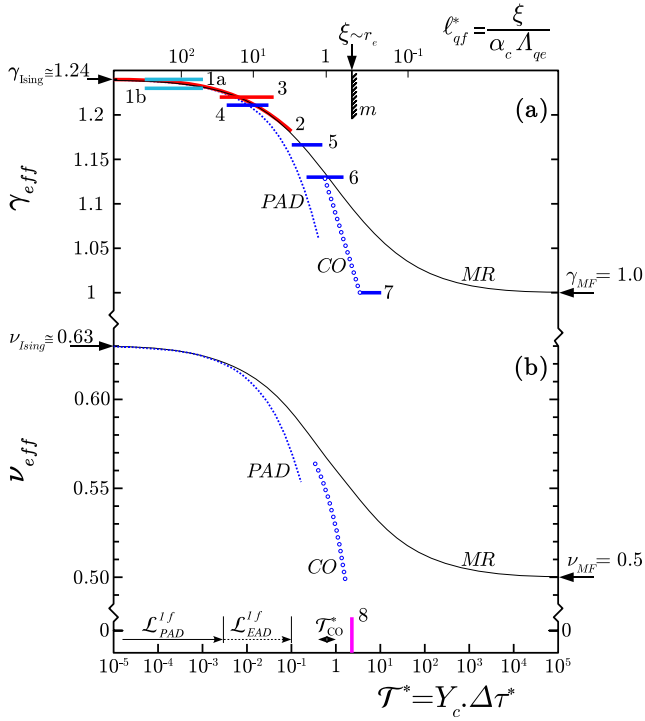


Figure 2: (Color on line) Variations of the effective exponents γ_{eff} (part a) and ν_{eff} (part b) as a function of the renormalized thermal field \mathcal{T}^* (lower axis) or as a function of the renormalized correlation length ℓ_{qf}^* (upper axis). The full curves labelled *MR* represent the γ_{eff} and ν_{eff} theoretical variations obtained from the respective mean crossover functions (see Ref. [34] and text). The dashed curves labelled *PAD* correspond to the exponent variation in the preasymptotic domain obtained from a Wegner expansion restricted to the first confluent correction [see equation (21) and text], whose thermal field validity extends up to $\mathcal{L}_{PAD}^{1f} \lesssim 3 \cdot 10^{-3}$ (see the corresponding arrow in \mathcal{T}^* axis). In the extended asymptotic domain (labelled *EAD*), the experimental master behavior is well-represented by the theoretical crossover function [see equation (31)], whose thermal field validity extends up to $\mathcal{L}_{EAD}^{1f} \lesssim 0.1$ (see the corresponding arrow in \mathcal{T}^* axis). The schematic curves labelled *CO* and the curve 8 (part b) correspond to the hypothesized *effective* crossover for pure fluids in a thermal field range $0.5 \lesssim \mathcal{T}_{CO}^* \lesssim 1$, (see the corresponding double arrow in \mathcal{T}^* axis). The 1-to-7 curves for γ_{eff} -variations refer [see also Ref. ([33])] to experimental estimations of the isothermal compressibility for xenon: 1a and 1b) from interferometric measurements (see Refs. [35] and [36], respectively); 2) from light scattering measurements (see Ref. [2]); 3) from turbidity and light scattering measurements (see Ref. [13]); 4-to-7) from pVT measurement analysis (see Refs. [13, 14, 37]). For the selected pVT measurements see Refs. [38, 39, 40]. For curve *m* see the Figure 1 legend and text.